Investigation of Impact Damage in Multi-Directional Tape Laminates and its Effect on Local Tensile Stiffness

R. Craven, P. Sztefek, R. Olsson

Investigation of Impact Damage in Multi-Directional Tape Laminates and its Effect on Local Tensile Stiffness

R. Craven, P. Sztefek, R. Olsson

PII: S0266-3538(08)00186-3
DOI: 10.1016/j.compscitech.2008.05.008
Reference: CSTE 4076

To appear in: *Composites Science and Technology*

Received Date: 20 November 2007
Revised Date: 29 April 2008
Accepted Date: 2 May 2008

Please cite this article as: Craven, R., Sztefek, P., Olsson, R., Investigation of Impact Damage in Multi-Directional Tape Laminates and its Effect on Local Tensile Stiffness, *Composites Science and Technology* (2008), doi: 10.1016/j.compscitech.2008.05.008

Investigation of Impact Damage in Multi-Directional Tape Laminates and its Effect on Local Tensile Stiffness

R. Craven[1]*, P. Sztefek[1] and R. Olsson[1]

[1] Department of Aeronautics, Imperial College London, Prince Consort Road, South Kensington, London, SW7 2AZ. UK. +44 (0) 20 7594 5087

* Corresponding author. E-mail address r.craven06@imperial.ac.uk

Abstract

This paper examines the effect of impact damage on local tensile stiffness of multi-directional tape laminates. A finite element model is used for parametric studies of the effect of various patterns of delaminations and cracks across the fibres. Regular and random crack patterns are considered for eight and sixteen ply quasi-isotropic laminates. The effect on local stiffness is evaluated by a recently developed inverse numerical approach. It is found that fibre cracks control the loss of stiffness but that delaminations are instrumental in extending the zone influenced by these cracks. Fractographic observations are finally used to generate a detailed model of the damage in a real laminate. A close agreement was found between the predicted and measured strain fields and the corresponding stiffness distributions obtained with the inverse method.

Keywords: A. Carbon Fibres, A. Laminate, B. Mechanical Properties, C. Finite Element Analysis (FEA) D. Inverse Method

Introduction

Impact damage is a constant concern in the design of structures of composite materials, and frequently controls the allowable strains [1]. The largest effects are normally seen in compression, primarily due to the interaction of delaminations and local buckling.

Tensile stiffness reductions have mainly been linked to fibre fracture and some authors have suggested that the region with fibre fracture may be regarded as a hole [2]. Others have suggested modelling the fibre damage zone as a soft inclusion [3]. The latter paper used laminate theory to calculate the inclusion stiffness, assuming zero stiffness of plies with broken fibres. An elementary finite element (FE) model of an impact damage in an 18 ply laminate under compression was presented in [4], where the damage was modelled as a single rectangular delamination and a number of cracks perpendicular to the loading direction. However, the appropriate stiffness distribution in the damage zone remains unclear. It should be noted that a detailed description of the stiffness gradients is crucial for determination of the stress concentrations and strength reductions caused by impact damage.

An early experimental study of fibre damage in impact damage zones was done by observing the tensile strength variation of fibre bundles within the damage zone [5]. Tensile tests on coupons taken from different parts of the damage zone have indicated that the stiffness reductions are non-uniform, non-zero and concentrated to a small central damage region with fibre fracture, [6]. A recent study used an inverse numerical method to evaluate experimentally measured displacement fields in impacted specimens, [7]. The predicted stiffness distribution confirmed the observations in [6].

The current paper presents a numerical study of the influence of impact damage on the local tensile stiffness of multi-directional laminates. Different patterns of fibre cracks and delaminations are included in a detailed Finite Element (FE) model of uniaxially loaded laminates. The corresponding local stiffness is evaluated using the inverse numerical approach in [7]. The models are validated by comparing the predicted strain fields with measurements on impacted laminates.

Initial Parametric Studies

The initial studies were inspired by the investigations of Olsson et al. [8] who conducted tensile stiffness evaluation of specimens with artificial impact damage. That gave a starting point for the study and motivated the use of the inverse method as verification of the FE results. The star crack pattern in [8] was generated by creating a cut perpendicular to the fibres in each ply prior to lay-up, producing a star crack pattern upon lay-up. This pattern was expected to give a large stiffness reduction in tension but the experimental results did not show this. This was felt to be a good starting point for a study into the effects of impact on tensile stiffness reduction. A parametric study of these star fibre fracture cracks was conducted using FE modelling to determine the parameters that controlled the stiffness reduction. These were constructed of 8 ply $(90/-45/+45/0)_s$ laminates 100 x 20 x 2 mm with single 18 mm fibre fracture cracks perpendicular to the fibres in each ply. They were modelled using brick elements with each ply being one brick thick. The study looked at an undamaged laminate, a laminate with fibre fracture cracks only, a laminate with delaminations only and a laminate with fibre fracture and delaminations. It was found that delaminations alone had no effect on the stiffness of the laminate in tension and that fibre fractures alone caused minimal average reduction in stiffness (12%), whereas delaminations combined with fibre fracture resulted in significant average stiffness reduction (55%). From this it was concluded that delaminations and fibre fracture are required to be present for stiffness reduction to occur in tension. This model of delamination and fibre fracture was also tested for eight different lay-ups $(0/-45/+45/90)_s$, $(0/90/+45/-45)_s$, $(90/0/-45/+45)_s$, $(90/-45/0/+45)_s$, $(+45/-45/90/0)_s$, $(+45/90/-45/0)_s$, $(-45/90/0/+45)_s$ and $(-45/0/90/+45)_s$. No difference between stiffness reductions in lay-ups with the same face ply orientation

was observed and very little variation was observed between laminates with different face ply fibre orientations.

These results are confirmed by the experimental findings in [8], where quasi-isotropic laminates with artificial star shaped fibre damage were tested. The resulting strain concentrations were found to be negligible at low applied strains, although strain concentrations appeared in the vicinity of the cracks as they opened and delaminations developed.

Full Scale Damage Models

For the full scale models combinations of different delamination patterns and fibre crack patterns, Fig. 1, were considered. In order to alleviate any problems with edge effects or hour-glassing of elements due to large deformation between the fibre fractures and the edge of the laminate, the laminate size was increased to 100 x 80 mm, with the damage located centrally. The laminate is an 8 ply quasi-isotropic balanced laminate with $(90/-45/+45/0)_s$ lay-up, nominally 2 mm thick. Having proven the stiffness reduction to be independent of lay-up sequence this lay-up was used because the fibre fracture cracks on the 90º plies do not open during loading. This provides a surface free from strain discontinuities from which the strain field can be measured, which is desirable to obtain good results from the inverse method.

There are four different delamination patterns as seen in Fig. 1a. These were chosen from the literature to investigate the differences in stiffness reduction caused by each, the circular delamination is the most basic and widely used [9], the twin ellipse pattern was proposed by Davidson [10], the peanut or lemniscates by Cairns [11], and finally the split peanut suggested by Hull and Shi [12].

The crack patterns in Fig. 1b include some patterns suggested in the literature as well as some random patterns generated in the present study. The star pattern from [8] assumes the cracks occur perpendicular to the fibres in each ply. The line cracks, which only occur in 0º plies, represent the model of stiffness reduction in [13], where it is assumed that the stiffness reduction can be modelled by failure in the 0º plies only. The three random distributions of cracks were generated using a Matlab® script, which randomly assigns a fibre fracture crack length between 1 mm and 15 mm positioned perpendicular to the fibre orientation inside an 18 mm diameter circle, and places between one and three cracks per ply. To compare the crack patterns a dimensionless parameter of average crack density (Avg. CD) has been created based upon the parameter crack density ρ defined in [14], Eq. (1.1), where the sum of the half length $L/2$ of each crack in a ply is summed and divided by an area A. In the present case A is the area of the 18 mm diameter circle that can be seen in Fig. 1b surrounding each of the crack patterns. The average crack density (Avg. CD) was obtained by averaging the crack density ρ across all n plies in the laminate

$$Avg.CD = \frac{1}{n}\sum_{j=1}^{n}\left(\rho_j\right) \qquad where \quad \rho_j = \frac{1}{A}\sum_{i=1}^{m}\left(\frac{L_i}{2}\right)^2 \tag{1.1}$$

The relative average crack densities for all crack patterns can be seen in the comparison in Fig. 2.

In order to verify the findings of these models, a model of a real 16 ply laminate impacted at 7J [7] was created based on fractography of the real laminate. The fractography for this study was taken from [15] although the And-scan® images of delaminations were too poor to determine delamination shapes so peanut shapes of the

correct diameter were used instead. Furthermore, some of the fibre fracture cracks were missed in the original fractographic study in [15] and had to be determined from re-examination of the actual de-plied laminate. To replicate the experimental loading precisely, the boundary conditions were the far field displacements observed in the experiment by using optical measurements based on Digital Image Correlation (DIC). A second FE model was also produced using the same peanut delaminations. The real fibre fracture was, however, replaced by a star crack pattern to demonstrate that reasonable results can still be obtained by simplifying the damage, to a complexity that can be easily implemented in a model.

Modelling Technique

Finite element modelling was conducted using ABAQUS® 6.6. The laminates were created using linear 3D brick elements (C3D8R) with one brick per ply thickness. The ply properties were entered as engineering material properties and the material (fibre) orientation for each ply was then assigned separately. The material properties used in the parametric studies correspond to the carbon/epoxy system HTA/6376C as reported in [16]. They are E_{11} = 137 GPa, $E_{22} = E_{33}$ = 10.4 GPa, $G_{12} = G_{13}$ = 5.19 GPa, G_{23} = 3.9 GPa, $\nu_{12} = \nu_{13}$ = 0.3 and ν_{23} = 0.51. For the experimental model, the material properties used corresponded to the material properties of the experimental laminate, taken from [7]. These are E_{11} = 141 GPa, $E_{22} = E_{33}$ = 8.9 GPa, $G_{12} = G_{13}$ = 4.73 GPa, G_{23} = 2.9 GPa, $\nu_{12} = \nu_{13}$ = 0.3 and ν_{23} = 0.50.

The delamination shape is created as a sketch on the surface and then extruded through the ply so that delaminations for both faces of the ply appeared on both faces, which allows a uniform mesh through the thickness of the ply. Ideally the fibre cracks within

the ply should be described by two disconnected surfaces along a straight line. In models with one ply this was achieved by cutting the ply into two parts and using the tie command to join the ply parts on either side of the crack. In multiply models this was not feasible as the nodes along the joined edges would have been used in two separate tie commands which is not permitted within ABAQUS®. For this reason the ply cracks in multiply models were modelled as highly extended ellipses, having a crack length of 1-15 mm and a crack width of 0.001 mm, by using the cut out tool available in ABAQUS 6.6® CAE. The laminate is then created by tying the plies together. All sections on the face of a ply, apart from the delaminated area are defined as a surface and then adjacent surfaces are tied together using the tie surface command within ABAQUS®. Studies using single ply models showed very little difference in the strain field between the elliptical cracks and the ideal line cracks, making elliptical cracks acceptable. The same problem with common nodes prevented shell elements from being used to model individual plies as the nodes were common to both surfaces and could not be used to tie both sides of the ply into the laminate.

No contact constraints have been used between the delaminations in these models, although the delaminated areas were observed to move and intersect in the out of plane direction during the solution. Comparing a laminate without contact constraints and a laminate with contact constraints revealed only a 1% difference in stiffness reduction but a six fold increase in solution time for the laminate with contact constraints. Consequently contact constraints were considered unnecessary.

Inverse Method

The homogenised constitutive parameters of the laminates represented by FE models as introduced above were sought using the indirect inverse method based on iterative updating of the material properties in an FE model using shell elements with a number of piecewise homogeneous zones [7]. The strategy is to minimise the difference between the displacements numerically predicted in the piecewise homogeneous FE model and the displacement fields obtained by solving the FE models with damage and stacked plies. As the inverse method is usually coupled with full field measurements obtained by Digital Image Correlation (DIC), the input (reference) displacements from the FE laminates with discrete damage features are considered only on the surface of the models. The iterative FE analyses of the piecewise homogeneous model, performed with the commercial software ABAQUS®, provide an updated displacement field resulting from a specific set of material parameters. The difference of these two displacement fields is denoted as displacement error and this error is minimised by employing The Steepest Descent optimization method. The basic principle of the inverse method is illustrated in Fig. 3.

The method has earlier been validated on numerical test cases using an isotropic FE model with artificial impact damage [7]. The Young's modulus and the Poisson's ratio were determined accurately when considering an "academic" displacement field without noise and were in a very good agreement when adding white noise to the reference displacement field. The method was then applied to DIC measurements on experimentally impacted laminates and the material properties were determined.

Stiffness Evaluation

The inverse method was applied to the FE models with an artificial damage created by coupling 5 different types of fibre fracture (star and line pattern, and random light, medium and severe cracks) together with 6 delamination types (circular delamination with radius of 10, 20 and 30 mm, twin ellipse, peanut and split peanut shapes having outer radius of 30 mm), see Fig. 1. The delaminations were orientated so that the major axis was aligned along the fibre direction of the lower ply, seen in Fig. 1c, as observed experimentally when examining impacted laminates [16]. The FE models were subjected to tensile load resulting in an applied strain of 0.3%, which had been selected not to exceed the elastic range of the material. Having different types of delaminations with outer radii 10, 20 and 30 mm, and fibre fracture concentrated within an 9 mm radius circle, it was decided to model the piecewise homogeneous FE model with the damage discretised into 6 sections to evaluate stiffness distribution with a reasonable resolution. As seen from previous studies [6] and [8], as well as from in-house experiments, the damage in quasi-isotropic laminates is fairly circular and therefore 5 mm wide concentric rings, positioned in the centre of the model were considered, Fig. 4. The outer radius of the damage region was then 30 mm. As the lay-up of the FE model is quasi-isotropic, the constitutive parameters for each section are limited to the Young's modulus and the Poisson's ratio. Both properties are sought as dimensionless relative values with respect to the undamaged material. A full convergence to the results being presented in this paper is achieved at typically about 50 iterations (about 2.5 hours using a Pentium® 4 CPU, 2.8 GHz). The elastic constants determined are plotted as normalised values (with respect to the undamaged material) across the width of the investigated sample through the centre of damage region, e.g. Fig. 5.

The results of peak and average stiffness for the different combinations of delamination shape and fibre fracture crack patterns are shown in Table 1. Not all delamination shapes were modelled with all fibre fracture crack distributions so where a model was not produced there is no entry in the table. Where a particular result is of interest it is identified with roman numerals I – XIII and are referred to in the following text. Result I from Table 1, is the control case with undamaged material, no delaminations and no fibre fracture cracks. Results II and III illustrate the stiffness reduction for line and star fibre fracture crack distributions without delamination; this stiffness reduction was found to be very localised. Results IV and V demonstrate that delamination alone causes no stiffness reduction in tension. Fig. 5 shows results VI – VIII which indicate that fibre fracture crack distributions combined with circular delaminations cause significant stiffness reduction. However, the predicted stiffness distribution only reflects the variation within the top ply, as the large circular delamination uncouples the displacements in the top ply from the remaining plies within the entire region where the local stiffness is evaluated. Consequently a delamination pattern which retains the coupling between the plies- as observed in real specimens and seen in the literature- is necessary. In Fig. 6a the stiffness reduction can be seen for the star and line fibre fracture crack distributions without delaminations (II, III). Fig. 6b shows the same fibre fracture crack distributions for peanut delaminations (IX, X), clearly showing that delaminations result in a more widespread stiffness reduction.

Fig. 7 proves that the stiffness reduction for the twin ellipse (XI), peanut (XII) and split peanut (XIII) models are very similar. Finally in Fig. 8 the comparison of the peak and average stiffness reductions for all different fibre fracture distributions is shown for the peanut delamination pattern. The trend is that as crack density increases the stiffness

decreases although this is not true for the moderate damage case. This, however, is a result of the cracks being more evenly distributed and not clustered in the centre. This creates a stiffer central region which is detected by the inverse method but offers no increase in structural integrity as it is surrounded by damaged material, resulting in an artificially high prediction of structural stiffness.

Experimental Comparison

The experimental comparisons in Fig. 9 illustrate that a replica model of the observed damage can reproduce the average stiffness reduction seen in the experiment to within 21%. This shows that a combination of delaminations and fibre fractures is the dominant failure mode in tension. The stiffness in Fig. 9 for the idealised model of peanut shaped delaminations with star pattern fibre fracture cracks is within 12% of the experimental results. This idealised model validates the work done in the parametric studies and demonstrates that such a model can be used to replicate impact damage in tension. It can easily be implemented for any stacking sequence or number of plies, based upon the delamination diameter obtained from C-Scan.

Discussion

The results in Table 1 clearly illustrate that delaminations without fibre fracture do not cause any tensile stiffness reduction. When fibre cracks are present the region with stiffness reduction is very small unless the fibre cracks are accompanied by delaminations. This observation can be explained by considering the shear lag effect, which causes a gradual recovery of stresses at some distance from a stress free surface. The stress recovery due to intralaminar (in-plane) shear stresses is relatively slow, as the

characteristic decay length is of the order of the fibre crack length. In contrast, the recovery due to interlaminar (out-of-plane) shear stresses is very fast as the characteristic length is of the order of a ply thickness. This is illustrated by Fig. 10, which shows that the strain concentration is very local when fibre cracks are not accompanied by delaminations. Similar observations have been made experimentally in [8]. The presence of delaminations eliminates the influence of the interlaminar stresses in the entire delaminated area so that only the slow shear lag effect from intralaminar stresses remains. This explains how delaminations increase the range of influence of fibre cracks.

The plots in Fig. 6b also demonstrate that for quasi isotropic lay-ups the model in [13] for modelling tensile stiffness reduction, which only considers fibre fracture in zero degree plies, is incorrect. The stiffness reduction for the star distribution is significantly higher than for line distribution where only the 0º fibres have fibre fractures, which shows that fibre fracture in plies of all orientations is significant. The model from [13] would probably still be valid for laminates with a high percentage of 0º plies.

The peanut model was chosen as its delamination pattern is the closest match to fractography of delaminations for carbon fibre epoxy laminates observed in the literature, [17] and [12]. The other delamination patterns, such as the split peanut and double ellipse, are still relevant and could be more suitable for laminates made from different fibre or matrix materials.

The effect of crack placement on limiting stiffness reduction for the moderate damage in Fig. 5 is one that should be noted. It demonstrates that the distribution of the stiffness reduction must be studied and that the peak and average stiffness values cannot be relied upon alone. A similar effect, where a region of less damaged material occurs in the

centre, can also be seen in the split peanut and ellipse models, Fig. 7. Although this region is less damaged it does not contribute to the structural integrity of the laminate because it is surrounded by damaged material. Similar phenomena have been observed experimentally; see Figs. 17 and 18 in [7].

The comparison between the experiments, the replica model and the idealised model shows that the fundamental parameters causing stiffness reduction in tension for impact damage have been captured. It is probable that the replica could have achieved a closer match to the experiment had better fractographic images of the delamination patterns been available, or if matrix cracks and initial imperfections in the laminate had been included. These factors contribute to the stiffness reduction although the effect is likely to be small. It is important to remember that the experiment is based on results from only one sample due to limited available data, and more importantly that the aim was to produce a method of modelling impact damage under tension load rather than replicating one particular case exactly. To this end a successful idealised model has been produced that replicates the impact damage stiffness reduction. It can easily be applied to any lay-up or thickness only requiring knowledge of the lay-up and the diameter of the delamination area determined from C-scan, which allows the size of the peanuts to be determined. The length of the fibre fracture cracks for the star pattern can be assumed to be approximately 50% of the delamination diameter [16]. This approach can be tailored to suit a particular laminate with further investigation using fractographic techniques or with prior knowledge of the typical delamination shape and the extent of the fibre fracture cracks in a particular laminate.

Conclusion

In conclusion, the important parameters of impact damage under tensile loading have been identified as fibre fracture cracks and delaminations in combination rather than simply fibre fracture cracks. Fibre fracture cracks in plies of all fibre alignments have been demonstrated to be important rather than just cracks in the zero degree plies, as previously thought.

An idealised model based on peanut shaped delaminations with a star pattern distribution of cracks has been developed and has been shown to provide a good approximation of the behaviour of impact damage observed in experiments. This model can be produced with knowledge of only lay-up and delamination diameter obtained from C-scan, although better results would be obtained by tailoring the delamination shapes to suit the laminate being modelled and with detailed fractographic information about the extent of fibre fracture cracks within the impact damaged laminate.

Acknowledgements

This project is funded by EPSRC in UK under grants GR/T18783/01 and EP/C531590/1 with CASE support from Airbus UK. The authors would like to thank Dr. Brian Falzon, Department of Aeronautics at Imperial College London and Dr. Matt Jevons, industrial supervisor of Airbus UK, for their help and support with this research.

References

1. Davies GAO, Olsson R. Impact on composite structures. The Aeronautical Journal 2004;108(1089):541-563.
2. Chamis CC, Ginty CA. Fiber composite structural durability and damage tolerance: simplified predictive methods. Composite Materials: fatigue and fracture (ASTM STP 1012). Philadelphia, PA, USA: ASTM, 1989. p. 338-355.
3. Cairns DS, Lagace PA. Residual strength of graphite/epoxy and kevlar/epoxy laminates with impact damage. Composite Materials: testing and design (ASTM STP 1059). Philadelphia, PA, USA: ASTM, 1990. p. 48-63.
4. Pavier MJ, Clarke MP. Finite element prediction of the post-impact compressive strength of carbon fibre composites. Compos Struct 1996;36(1):141-153.
5. Elber W. Failure mechanics in low-velocity impacts on thin composite plates (NASA TP-2152). Hampton, VA, USA: NASA, 1983.
6. Sjögren A, Krasnikovs A, Varna J. Experimental determination of elastic properties of impact damaged in carbon fibre/epoxy laminates. Composites Part A 2001;32(9):1237-1242.
7. Sztefek P, Olsson R. Tensile stiffness distribution in impacted composite laminates determined by an inverse method. Composites Part A 2007; in press doi:10.1016/j.compositesa.2007.10.005
8. Olsson R, Iwarsson J, Melin G, Sjögren A, Solti J. Experiments and analysis of laminates with artificial damage. Compos Sci Technol 2003;63(2):199-209.
9. Abrate S. Impact on laminated composite materials. Appl Mech Rev 1991;44(4):155-190.

10. Davidson BD. On modelling the residual strength of impact damaged compression loaded laminates. Advanced Materials: The Big Payoff Conference Proceedings, Atlantic City, NJ, USA: SAMPE, 1989. p. 109-119.

11. Cairns DS. Impact and post impact response of graphite/epoxy and kevlar/epoxy structures (TELAC Report 87-15). Cambridge, MA, USA: Massachusetts Institute of Technology; 1987.

12. Hull D, Shi YB. Damage mechanism characterisation in composite damage tolerance investigations. Compos Struct 1993;23(2):99-120.

13. Cairns DS, Lagace PA. Residual strength of graphite/epoxy and kevlar/epoxy laminates with impact damage (ASTM STP 1059). Philadelphia, PA, USA: ASTM;1990.p. 48-63.

14. Shen L, Li J. A numerical simulation for the effective elastic moduli of plates with various distributions and sizes of cracks. Int J Solids Struct 2004;41(26):7471-7492.

15. Gamelin A. Observation of impact damage zones. MSc Thesis, ENSICA, Imperial College London, Department of Aeronautics 2007.

16. Sjögren A. Fractographic characterization of impact damage in carbon fibre/epoxy laminates (FFA TN 199-17). Bromma, Sweden: The Aeronautical Research Institute of Sweden; 1999.

17. Levin K. Characterisation of delamination and fibre fractures in carbon fibre reinforced plastics induced from impact. Mechanical Behaviour of Materials Conference Proceedings, Kyoto, Japan: Pergamon Press, 1991. p. 519-524.

Figure Captions

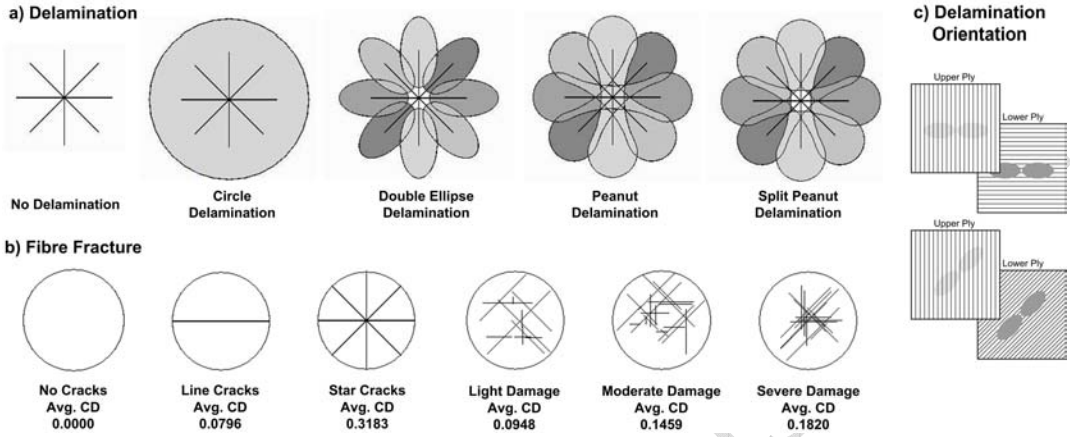

Figure 1 a) Delamination patterns, b) Fibre fracture patterns and average crack densities, c) Delamination orientation with respect to ply fibre direction

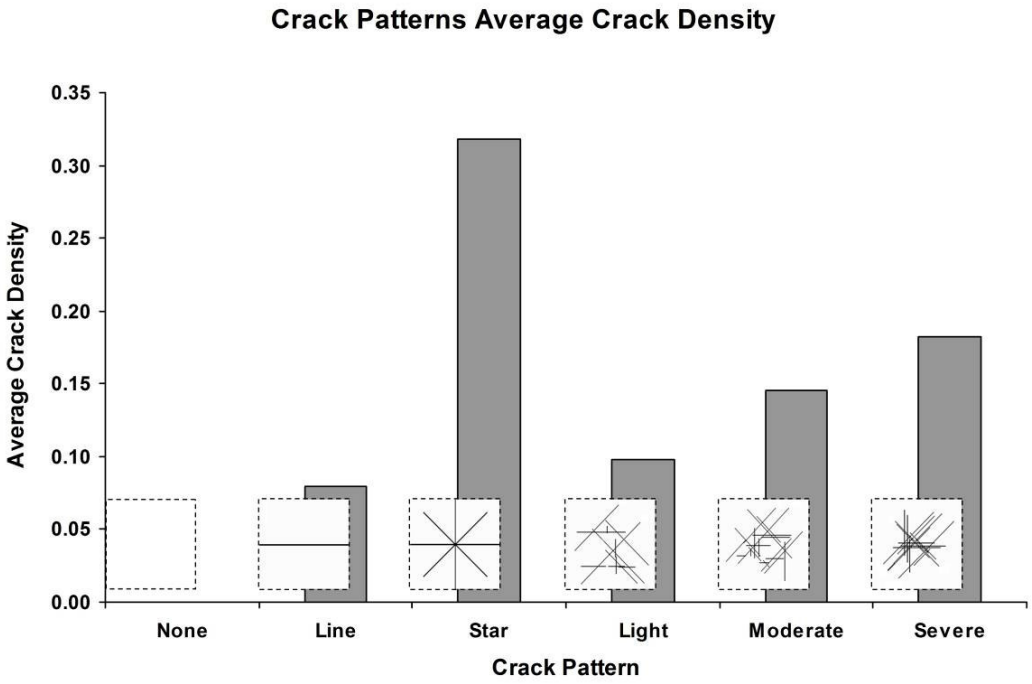

Figure 2 Average crack densities for crack patterns

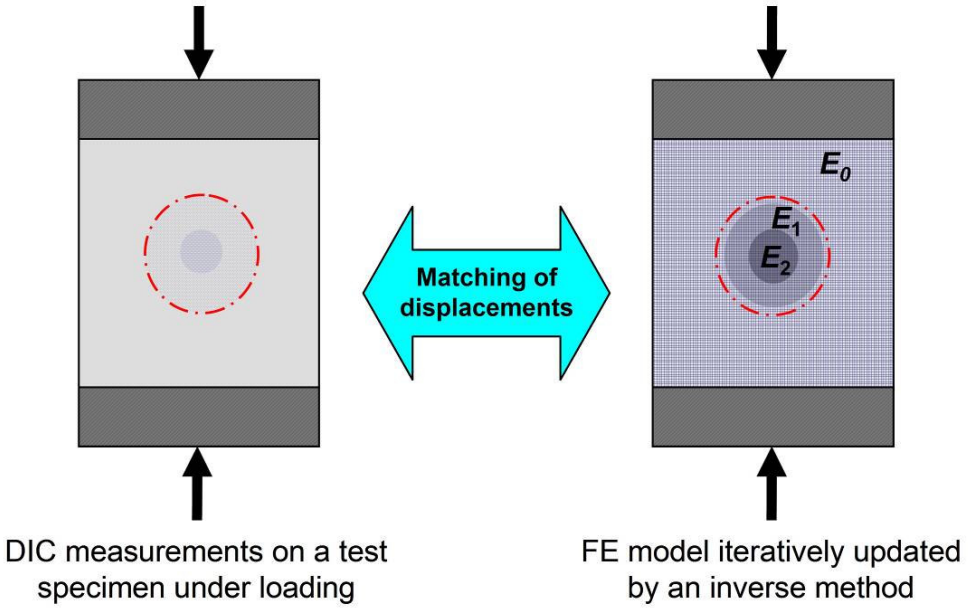

Figure 3 The fundamentals of the inverse approach

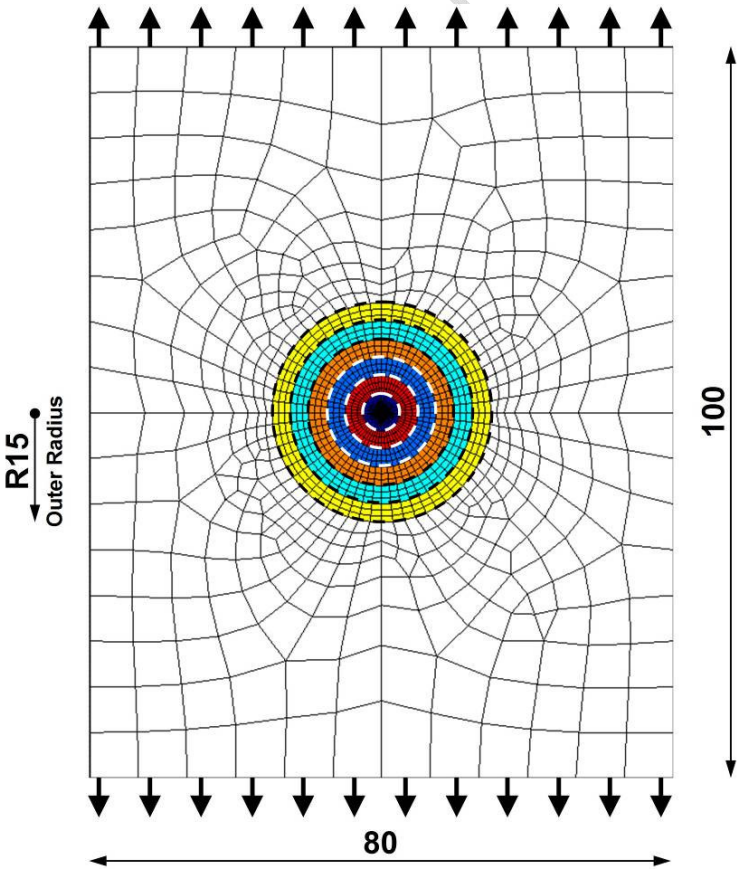

Figure 4 Discretisation of the piecewise homogeneous FE Model

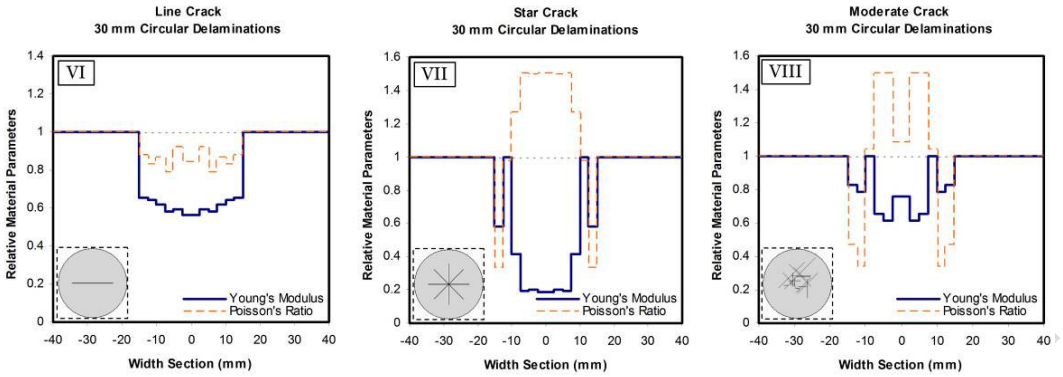

Figure 5 Circular delaminations with different fibre fracture crack patterns

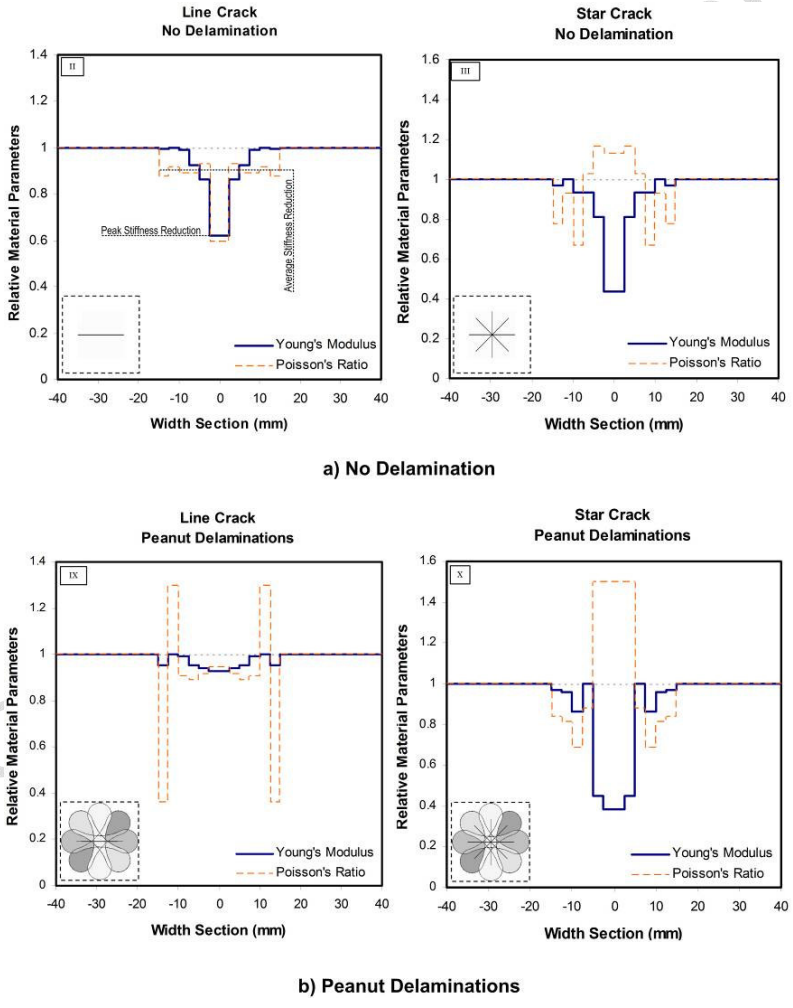

Figure 6 a) Star and line crack stiffness reduction without delamination b) Star and line crack stiffness reduction with peanut delaminations

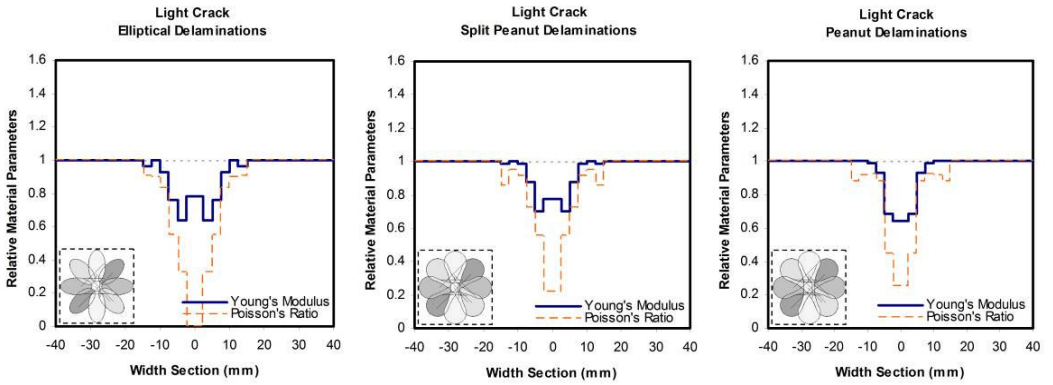

Figure 7 Stiffness reductions for three different delamination patterns, all with light fibre fracture crack distributions

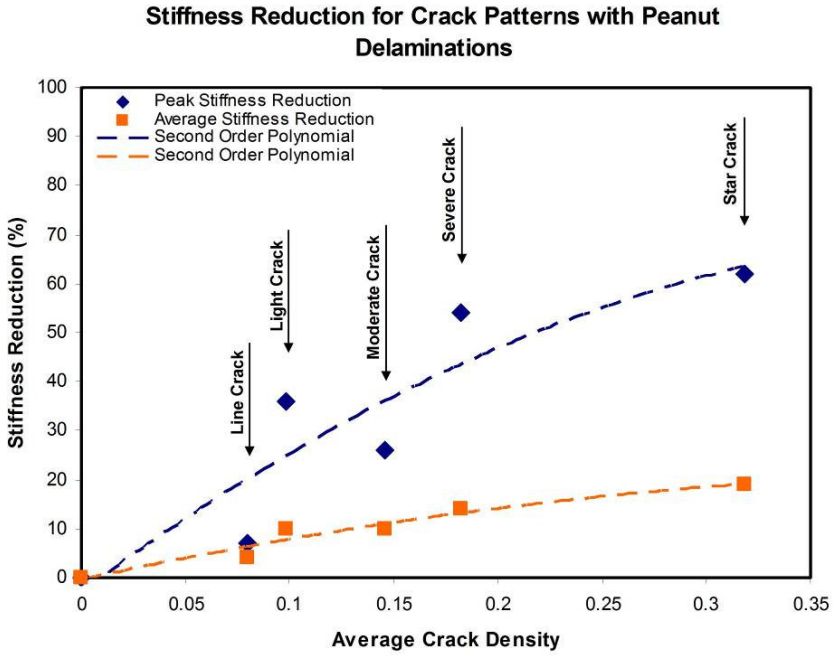

Figure 8 Peak and average stiffness reductions for all fibre fracture crack distributions with peanut delaminations

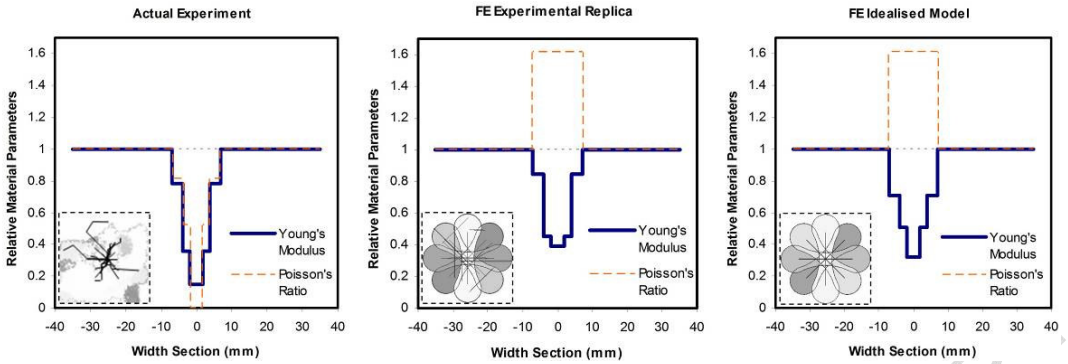

Figure 9 Stiffness reductions in actual experiment, FE replica and FE model

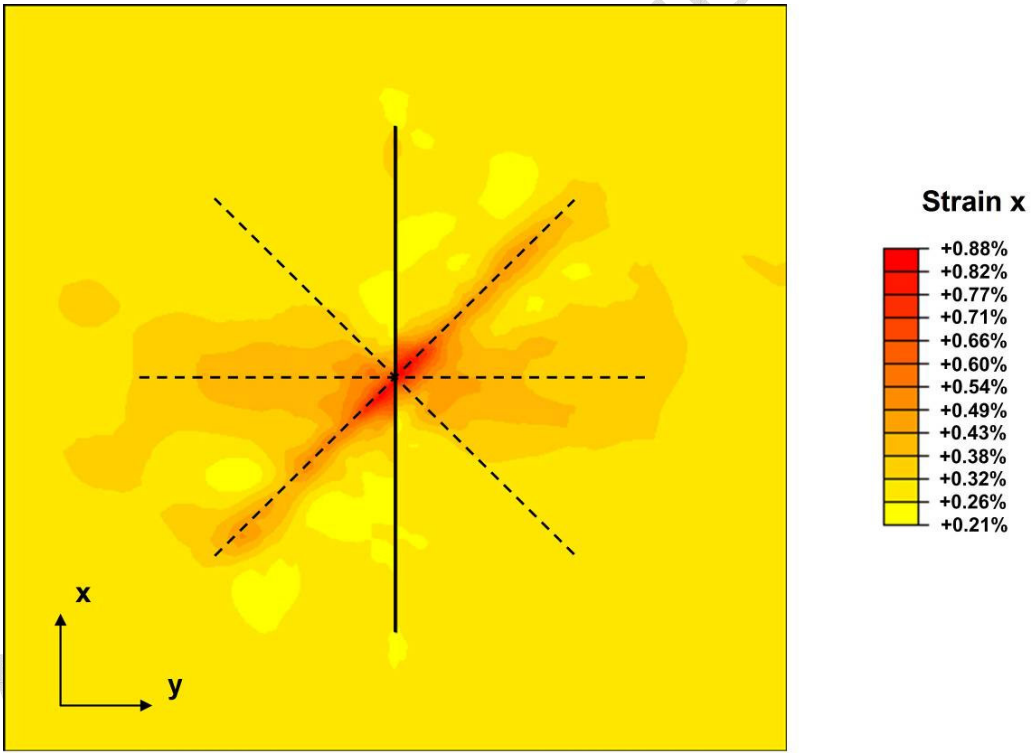

Figure 10 Shear-lag effects on strain distribution of star fibre fracture crack distribution with no delamination

Tables

Table 1 Stiffness reductions for all crack patterns and delamination shape combinations studied

Percentage Peak (Average) Stiffness Reduction		Cracks					
		None	Line	Star	Light	Moderate	Severe
Delaminations	None	I 0 (0)	II 38 (8)	III 57 (12)	15 (5)	14 (3)	30 (6)
	10 mm Circle		56 (19)	98 (27)		55 (16)	
	20 mm Circle		55 (37)	88 (54)		43 (24)	
	30 mm Circle	IV 0 (0)	VI 44 (39)	VII 81 (55)		VIII 39 (23)	
	Twin Ellipse		34 (7)	56 (17)	XI 36 (15)	29 (9)	39 (9)
	Split Peanut		9 (3)	48 (15)	XII 30 (10)	24 (7)	30 (9)
	Peanut	V 0 (0)	IX 7 (4)	X 62 (19)	XIII 36 (10)	26 (10)	54 (14)